LANGMUIR

pubs.acs.org/Langmuir Article

Colloidal Engineering of Microplastic Capture with Biodegradable Soft Dendritic "Microcleaners"

Rachel S. Bang,[#] Lucille Verster,[#] Haeleen Hong, Lokendra Pal, and Orlin D. Velev[*]

Cite This: *Langmuir* 2024, 40, 5923−5933 Read Online

ACCESS | Metrics & More | Article Recommendations | Supporting Information

ABSTRACT: The introduction of colloidal principles that enable efficient microplastic collection from aquatic environments is a goal of great environmental importance. Here, we present a novel method of microplastic (MP) collection using biodegradable hydrogel soft dendritic colloids (hSDCs). These dendritic colloids have abundant nanofibrils and a large surface area, which provide an abundance of interfacial interactions and excellent networking capabilities, allowing for the capture of plastic particles and other contaminants. Here, we show how the polymer composition and morphology of the hSDCs can impact the capture of microplastics modeled by latex microbeads. Additionally, we use colloidal DLVO theory to interpret the capture efficiencies of microbeads of different sizes and surface functional groups. The results demonstrate the microplastic remediation efficiency of hydrogel dendricolloids and highlight the primary factors involved in the microbead interactions and adsorption. On a practical level, the results show that the development of environmentally benign microcleaners based on naturally sourced materials could present a sustainable solution for microplastic cleanup.

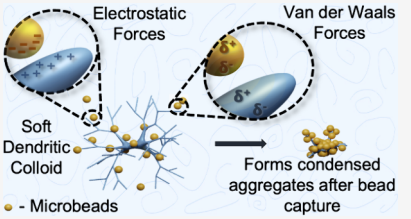

INTRODUCTION

The boom of plastic production and increasing consumer demand for industrial products has accelerated worldwide microplastic (MP) accumulation at a startling rate.[1−8] Millions of tons of discharged plastic are accumulated within the ocean floors and surface.[9−11] MPs have been described as a plurality of mostly particulate contaminants[12] that can potentially be a significant risk to the environment[3,13−15] and human health.[3,8,16−18] They are one of the few global environmental change (GEC) factors that are both physical and chemical in nature.[19] MPs are loosely defined as plastic particles of less than 5 mm. More recently, they have been designated with a lower limit of 100 or 1000 nm, below which these particles are considered nanoplastics (NPs).[20−22] In this Letter, we will use the term MP more broadly to encompass both MP and NP sizes.

Due to the colloidal size scale of MPs, there are fundamental changes in their behavior that differ from the corresponding macroscale properties.[15] For example, their size allows for faster transport by multiple mechanisms across the total environment, i.e., land, aquatic, and atmospheric ecosystems.[15,23,24] Additionally, the large surface area of MPs can inadvertently collect a variety of microorganisms, pathogens, and toxins, much more than particles of larger sizes, and can negatively impact the health of animals and humans that have ingested or inhaled the plastic particles.[12,14,22,25,26]

One major problem with MPs in the environment emerges from the fact that most collection and removal methods for large plastic waste cannot be used for MP particles due to their small size.[27−29] Many current techniques of MP separation are based on standard methods such as filtration and centrifugation. These techniques have scale-based efficiency limitations[30−33] and may be energy-intensive, time-consuming, and cost-prohibitive.[34] Techniques that target other MP characteristics, e.g., density, show promise but may be complicated to implement and lacking in throughput.[30] Ultimately, reducing and eliminating MPs in the environment relies on limiting single-use plastic products and replacing them with alternatives such as bioplastics.[35,36] However, even if such environmentally oriented technologies are adopted today, an enormous amount of synthetic polymers are already discarded in the environment and will release MP particles that will need cleanup for many years to come.

Designing novel MP capture solutions requires consideration of colloidal fundamentals since many MPs fall within the colloidal size range of 1 nm to 1 μm.[37] MP remediation methods based on interfacial interactions may be the key to efficient removal of MP from water. Coagulation and flocculation are methods that leverage surface interactions to separate suspended particles, including MPs, in wastewater treatment plants.[38−40] Despite their efficacy in particulate removal,[41] the use of chemical coagulants may be undesirable in many situations as a large amount of compound is required and it can be difficult to thoroughly remove the used coagulants from the water.[41,42] Overall, MP pollution is a pervasive problem that has been difficult to address.

Received: December 13, 2023
Revised: February 19, 2024
Accepted: February 21, 2024
Published: March 1, 2024

https://doi.org/10.1021/acs.langmuir.3c03869
Langmuir 2024, 40, 5923−5933

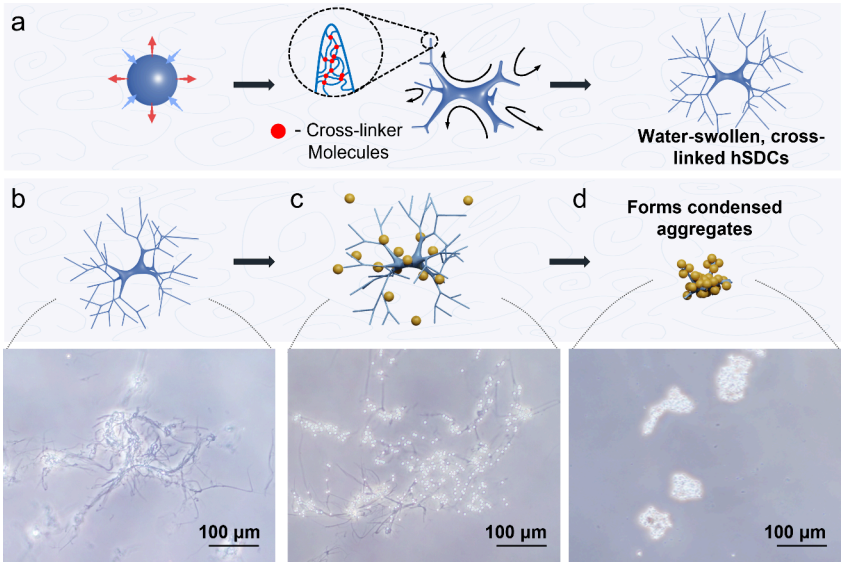

Figure 1. Overview of chitosan (CS) hSDC making and operation. (a) Schematic of hSDC formation through ionic cross-linking within turbulent flow. (b, c) Initially, latex microbeads are captured along the surface of the dendricolloids without significant conformational change. (d) As the CS hSDCs become saturated with microbeads, the hSDC-bead complex forms denser aggregates. Corresponding brightfield microscopy images of CS hSDC particles at different stages of microbead collection are shown at the bottom.

Here, we develop and test a new concept of MP collection that relies on polymer particle interfacial properties and interactions in order to capture model MP particles (Figure 1). Hydrogel soft dendritic colloids (hSDC) are produced through a multiphasic liquid shear-based fabrication technique within high-energy fluid-dissipative conditions (Figure 1a).[43] The hSDCs have a hyperbranched fibrous corona with individual fibers ranging in diameter from nanometer to tens of micrometers and having a large excluded volume, which endows them with properties advantageous in applications such as coatings, nonwovens, and rheological modifiers.[43−46] The abundant nanofibrils and their large surface area provide excellent networking capabilities[43,45] and a propensity for strong adhesion via van der Waals (vdW) forces and "contact splitting" (Figure 1b).[43] As shown in detail here, these characteristics give them the potential to capture a significant number of particulate contaminants from polluted water. The mechanisms of MP capture investigated here are based on interfacial interactions, which are abundant due to the hSDC's large surface area and fewer size-based limitations than conventional methods.

The need to perform the capture and environmental remediation of MPs from natural water bodies leads to additional restrictions on the type of material that can be used for hSDC "microcleaners". Given that some of the hSDCs could remain dispersed in the aquifers, they need to be made from biodegradable polymers, allowing for the degradation of residual hSDCs into natural byproducts. Thus, the majority of experiments reported here were performed with hSDCs produced from two bioderived and biodegradable polymers following the methods in Williams et al. (Supporting Information (SI) Figure S1a,b).[45] The first one is chitosan (CS), a deacetylated form of chitin commonly derived from the exoskeletons of crustaceans.[47−51] CS is positively charged (Figure S1c) at lower-pH conditions and could find medical applications due to its antibacterial properties.[52] The second biopolymer is sodium alginate (SA), which is extracted from various brown seaweed species. It is used in a wide range of industries such as food packaging,[53] biomedicals, pharmaceuticals,[54,55] and adhesives[56] due to its gelation and film-producing capabilities. It is negatively charged across a range of pH conditions due to its carboxyl groups (Figure S1d).

We prepared samples of soft dendritic microcleaners and characterized their MP capture efficiency as a function of their morphology, polymer composition, and medium conditions. Commercial, surfactant-free, monodisperse polystyrene (PS) latex microbead dispersions were used as model MPs, the capture of which was evaluated under various salinity and pH conditions. In the course of data analysis, we initially investigated the feasibility of a simple particle packing model for predicting microbead adsorption. Then, we examined the Derjaguin−Landau−Verwey−Overbeek (DLVO) theory, which considers a combination of electrostatic double-layer and vdW forces,[57−59] for a potential interpretation of the interactions that promote microbead−SDC adhesion.

EXPERIMENTAL SECTION

Chemicals and Materials. The biopolymers used for synthesizing hSDCs were CS (low M_w, ∼77% deacetylated, Sigma-Aldrich) and SA (Sigma). Trisodium citrate dihydrate (NaCit) (Fisher) and calcium chloride ($CaCl_2$) (Sigma) were used as ionic cross-linkers for CS and SA, respectively. Acetic acid (HOAc) (Acros Organics) was diluted to 1.5% as a solvent for CS. Sulfonated PS (S-PS) latex microbeads (surfactant-free 0.82 and 1.8 μm microbeads from Thermo Fisher Scientific, 0.25 μm from Bangs Laboratories Inc.) and amidine-functionalized PS (A-PS) latex microbeads (1 μm from Thermo Fisher Scientific and 3.19 μm from Life Technologies) were used as model MPs. Sodium chloride (NaCl) was obtained from Sigma-Aldrich and was used for testing various ionic strengths. Hydrochloric acid (HCl) (Sigma-Aldrich) and sodium hydroxide (NaOH) (Sigma-Aldrich, reagent grade, ≥98%, anhydrous pellets) were used to adjust the pH of the samples.

Fabrication of Biodegradable CS and SA SDCs. Turbulent flow conditions were produced using a lab-scale colloidal mill (IKA Magic Lab with MK module, IKA Works, Germany) at speeds up to 26,000 rpm (approximately 433.3 s^{-1}). CS was dissolved in 1.5% HOAc and SA in water. The CS and SA solutions were injected directly into the shear zone of the colloidal mill and ionically cross-

https://doi.org/10.1021/acs.langmuir.3c03869
Langmuir 2024, 40, 5923−5933

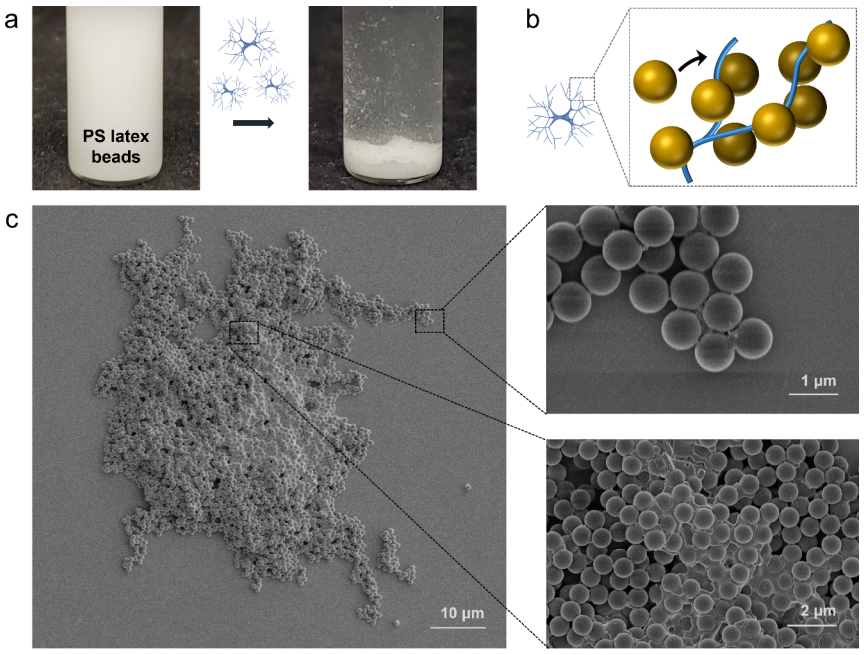

Figure 2. Capture and removal of sulfonated PS latex microbeads by CS hSDCs. (a) The hSDCs collect a significant number of microbeads from water and then sediment. (b) The microbeads are expected to pack tightly around the dendricolloid fibers. (c) SEM images of dry CS hSDC and microbead aggregates show how the beads can be captured by individual thin CS fibers (top) and fully enveloped by an SDC aggregate (bottom).

linked within turbulently sheared aqueous solutions of 25 mM NaCit and 13 mM $CaCl_2$, respectively. The collected hSDC particles were washed several times with deionized (DI) water before storage in DI water in a fridge. The dry weight percentages of the suspensions were determined by the weight differences between the wet and dry suspension weights. Water was removed or added to the suspensions to match the hSDC concentrations across the experiments.

Cylindrical hydrogel microrods were produced in less turbulent conditions by injecting of 3 wt % CS solution at 0.05 mL/min into NaCit solution stirred with a magnetic stir bar (200 mL of cross-linking medium in a 250 mL beaker, with a stir bar speed of 100 rpm). Hydrogel chunks were produced by homogenizing hSDCs (IKA Ultra-Turrax) at 12,000 rpm until broken into smaller pieces. CS particulate chunks were produced by physically grinding the CS powder with a mortar and pestle. CS particle samples of 0.15 mg dry weight CS were suspended in DI water with microbead concentrations ranging from 4.2×10^8 to 1.7×10^{10} microbeads/mL.

Imaging. Brightfield and fluorescence microscopy (Olympus BX-61) were used to confirm and characterize the dendritic particles and visually inspect the degree of microbead capture. Scanning electron microscopy (SEM, FEI Verios) was used to observe CS hSDC fiber entanglement around bead aggregates. Due to the exceptional thinness of the hSDC fibers after drying on the SEM sample stub, the samples were not sputter-coated.

Microbead Capture Tests and Evaluation of the Number of Captured Microbeads. Microbead dispersions of various concentrations were made from stock dispersions. These stock solutions were sonicated each time before being added to the experimental samples. During the experiments, most of the samples had a medium of pure DI water or 0.6 M NaCl to represent the natural salinity of the ocean.[60,61] In experiments where the effects of pH were investigated, no salt was added and the pH was adjusted with small volumes of HCl or NaOH solutions. The pH values of the samples ranged from 4 to 8.5.

The hSDCs in the form of aqueous suspensions were carefully pipetted into the samples with microbead dispersions. These samples were vortexed for ≈5 s to promote mixing and microbead adsorption. The samples were then allowed to settle. Stoke's law (SI 1.1) was used as a reference for a time frame in which to collect the supernatant, but after gravimetric separation, the supernatant was checked microscopically to ensure that no hSDC-bead aggregates were present. Once the supernatant was confirmed to contain "uncaptured" microbeads, approximately 300 μL of the supernatant was collected for absorbance measurements. The absorbance was measured using a plate reader (490 nm, Synergy MX multimode microplate reader, BioTek, Santa Clara, USA). Calibration curves were made to correlate absorbances with known concentrations of microbeads. The Beer–Lambert Law was used to determine the concentration of beads that are not captured by the hSDCs, and further details are described in Supporting Information (SI 1.2).

The microbead collection data have been normalized by the mass of microbeads collected versus the mass of polymer from the hSDCs. While the authors acknowledge that normalizing adsorption data by surface area is more informative, current methods make it difficult to estimate the hSDC surface area.

Zeta Potential Measurements. The zeta potentials of SDCs and latex microbeads were measured using a Nano Zetasizer (Zetasizer Nano ZSP, Malvern, UK) with a dip cell (ZEN1002, 2 mm electrode gap). The ionic concentration was 0.1 mM NaCl. The samples were set to a specific pH with dilute solutions of HCl and NaOH. The CS hSDC samples were freeze-dried and then redispersed in water. The solution was then homogenized at 12,000 rpm for 10 min to break the fibers into roughly spherical particles. Next, the homogenized suspension was washed with DI water and left to rehydrate and undergo a gravimetric separation fully. Finally, the smaller, less polydisperse hydrogel chunks near the top of the supernatant were collected and used for zeta potential measurements. Later on, additional zeta potential measurements were taken without freeze-drying to ensure that freeze-drying and rehydration of CS did not affect the zeta potential measurements. All other tests measuring hSDC zeta potential were done without the freeze-drying step (Figure S1c,d).

RESULTS AND DISCUSSION

Experimental Setup and Choosing of the Initial SDC Polymer. The initial experiments focused on systems of negatively charged S-PS latex microbeads (0.82 μm diameter), to which we added small amounts of CS hSDCs. We observed that individual CS hSDCs, typically having a hierarchically

https://doi.org/10.1021/acs.langmuir.3c03869
Langmuir 2024, 40, 5923−5933

branched fibrillar structure of a couple of hundred microns in overall size,[43,45] and slight positive charge (made of CS with $pK_a \approx 6.5$) readily collect the suspended microbeads as the branches of the dendritic particle adhere to the microbeads. Due to the hSDCs' large, interconnected surfaces, individual dendricolloids form extensive networks, which "trap" the captured microbeads into the entangled fibers (Figure 1c). The heteroaggregation of latex beads and hSDCs eventually results in the formation of condensed aggregates (Figure 1d). These large microbead−hSDC clumps were easily separated from the uncollected "free" microbeads due to their rapid gravitational sedimentation (Figure 2a and SI 1.1).

The large surface area of the hSDCs allows for massive microbead capture on the dendritic fibers (Figure 2b). An SEM image of a large aggregate of S-PS and CS hSDCs, of one or potentially a few SDCs combined into one aggregate, is shown in Figure 2c. Microbeads near the center of the aggregate are seemingly trapped near the thicker CS backbone, while the microbeads near the periphery outline the branched fibers "bridging" the gaps between the microbeads. We estimate that this specific aggregate of hSDCs contains a minimum of ≈2000 captured beads. Thus, the hSDCs are shown to be a highly efficient means of polymer colloid collection and removal. A more detailed analysis of the aggregated and separated masses by SEM (Figure S2) reveals that most of the beads are captured on the SDC fibrils, although a few free beads are also present, likely as a result of being dragged down by the aggregates.

Next, we characterized the role of the material of the SDCs and the beads on the aggregation efficiency. These experiments included hSDCs of two compositions, CS and SA, as well as (nonhydrogel) SDCs from two common synthetic polymers, cellulose acetate (CA) and polystyrene (PS). These dendricolloids of different polymeric origins were introduced into concentrated suspensions of S-PS latex microbeads (Figure 3a). Initially, the CS hSDCs, which have positive ionic charges, were qualitatively observed to be most efficient in microbead collection (Figure 3a). Thus, we hypothesized that the electrostatic interactions were a major force of microbead adsorption onto the dendritic particles. However, the other slightly neutral or negatively charged dendricolloids captured some microbeads as well, albeit not at the same level of efficiency as CS hSDCs (Figure 3b). These observations suggest that vdW interactions are a major driving force for microbead capture by the SDCs. This is not surprising as vdW interactions were earlier found to play a crucial role in the adhesivity of SDCs.[43] Thus, the adsorption of polymer microparticles to the CS hSDCs is driven by the combined effect of attractive electrostatic and vdW forces.

Role of SDC Morphology in Microbead Capture. After confirming that CS hSDCs can serve as efficient microcleaners, we characterized the role of their morphology and gel-like characteristics on the capture efficiency. Several CS morphologies, including dendricolloids, cylindrical rods, precipitated chunks, and ground chunks, were fabricated as described in Experimental Section and shown in Figure 4a.

We found that the CS hSDCs and hydrogel chunks consistently had the highest microbead capture efficiencies across a range of initial bead concentrations (Figure 4b). The hydrogel rods did not perform consistently, which could be due to their lower surface area to volume ratio and a larger inherent polydispersity of the hydrogel rod suspensions that are a new material made by an ad-hoc procedure.[45] The

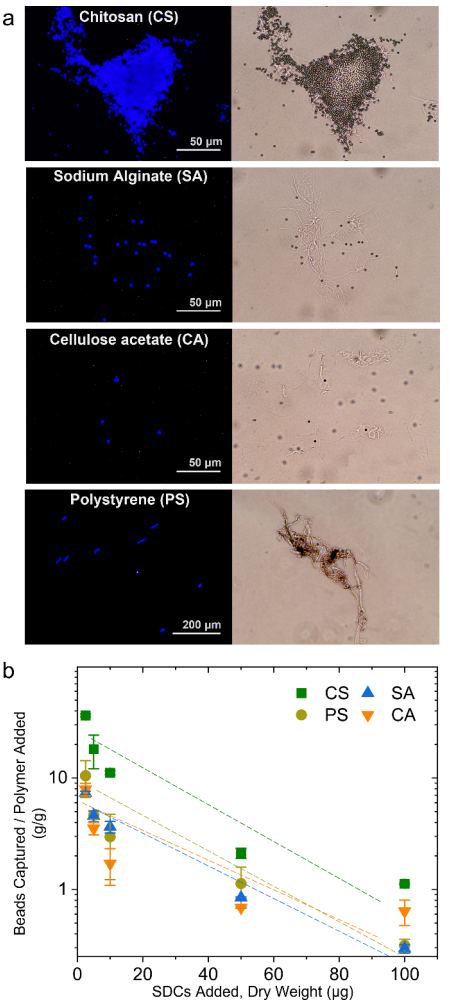

Figure 3. Polymer material used in the SDC microcleaners affects the efficiency of latex microbead capture. (a) Two biosourced hSDCs (CS and SA) and two synthetic polymer SDCs (CA and PS) were introduced to a microbead suspension and imaged after some time to determine the level of microbead capture. CS hSDCs outperform dendricolloids fabricated from different types of polymers. (b) Correlation between the mass of 0.82 μm sulfonated-PS microbeads captured per mass of the polymer (dry weight). Dotted lines follow the general data trends.

ground CS chunks did not perform well, especially at higher initial microbead concentrations (approximately 2.5-fold lower microbead capture per gram of dried CS than CS hSDCs at 11.3×10^9 microbeads/mL). This is likely because the "ground chunks" are finely grounded CS powder and are not considered a hydrogel, unlike the "chunks", which are smaller, nondendritic hydrogel particles fabricated through nonsolvent precipitation in the liquid shear-based technique. The lack of hydrogel characteristics may have led to a reduced adsorption efficiency. These observations suggest that the large surface area and excluded volume of the dendricolloids' nanofiber coronas are essential in microbead capture through interfacial adhesion and entanglement in the nanofibrils.

Identifying the Dominant Interactions in Microbead Adsorption. The initial results show that CS hSDCs are able to effectively capture microbeads even in solutions with high salt concentrations (Figure S3). Thus, our next goal was to identify and analyze the dominant interactions guiding microbead adsorption and capture. In these experiments,

https://doi.org/10.1021/acs.langmuir.3c03869
Langmuir 2024, 40, 5923−5933

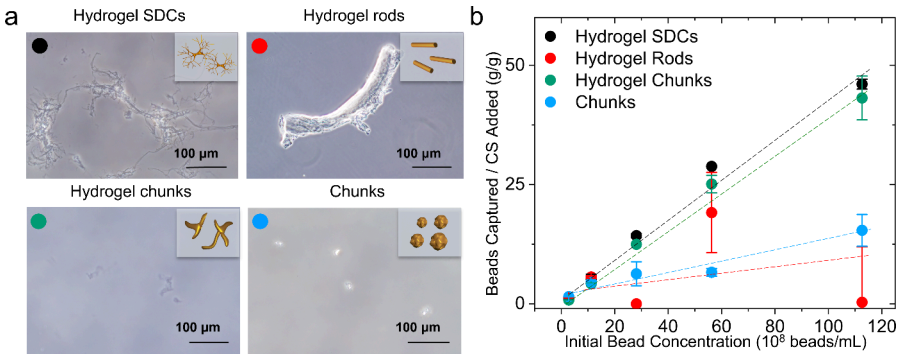

Figure 4. Morphology of CS and its hydration state (hydrogel and nonhydrogel) affect the performance of latex microbead capture (right graph). (a) Microphotographs of the four types of particles compared. (b) Greater performance is attributed to greater surface area in the CS hSDCs and the gel-like surface. Dotted lines follow the general data trends.

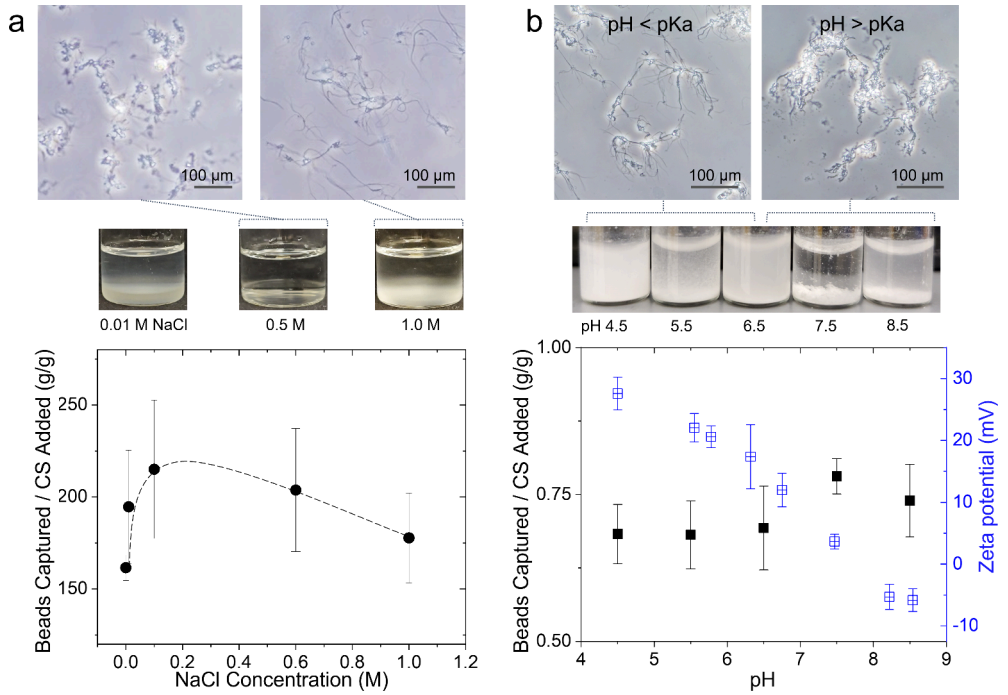

Figure 5. Ionic concentration and pH affect electrostatic interactions. (a) Despite the conformational changes in different ionic concentrations, there was no significant effect in the microbead collection. (b) Dendricolloid particle conformation changed with pH, leading to condensed agglomerates above the pK_a of CS. Microbead capture was slightly better at higher pH conditions, despite the agglomerated conformations. Note that approximately 300× more CS hSDCs were added to the samples for the pH variation experiments, resulting in smaller ratios of beads captured/CS. Dotted lines follow the general data trends.

approximately 5 μg (dry weight) of CS hSDCs was used in each sample. First, the role of electrostatic interactions was evaluated by varying the ionic concentration of the microbead suspensions. Increased salinity screens electrostatic interactions by decreasing the Debye length, a measure of how far a particle's net electrostatic charge will persist in the solution.[58] Initially, we expected that higher ionic concentrations would significantly reduce the degree of microbead adsorption since we hypothesized that the CS hSDCs would agglomerate in an ionic medium of approximately 0.6 M NaCl (a salinity similar to marine conditions)[60,61] due to surface charge suppression. However, the salinity of the medium did not significantly affect the number of microbeads captured by the hSDCs across a broad range of salt concentrations (Figure 5a). Additionally, control experiments were done in varying salinities with only microbeads and no SDCs added and it was found that the percentage of sedimented microbeads was relatively small compared to samples aggregated with SDCs and with much smaller aggregates of the beads (Figure S4).

One other notable observation in the ionic media variation experiments was the SDC fibril re-expansion at high salinity (top images of Figure 5a), which was unexpected, as the charge is expected to be diminished at high ionic strengths. However, a theoretical study by Moncho-Jordá et al. predicts an inversion of particle net charge in microgels.[62] Specifically, this occurs when short-range interactions between the counterions and the charged microgel polymer chains enhance counterion adsorption on the surface, which may provide one possible explanation for why the CS hSDCs adopt an expanded conformation under high salt conditions (Figure 5a). Regardless, the sustained performance of CS hSDCs suggests a predominant contribution from vdW forces to microbead adsorption, which ensures MP capture in high-salinity environments such as oceans.

https://doi.org/10.1021/acs.langmuir.3c03869
Langmuir 2024, 40, 5923−5933

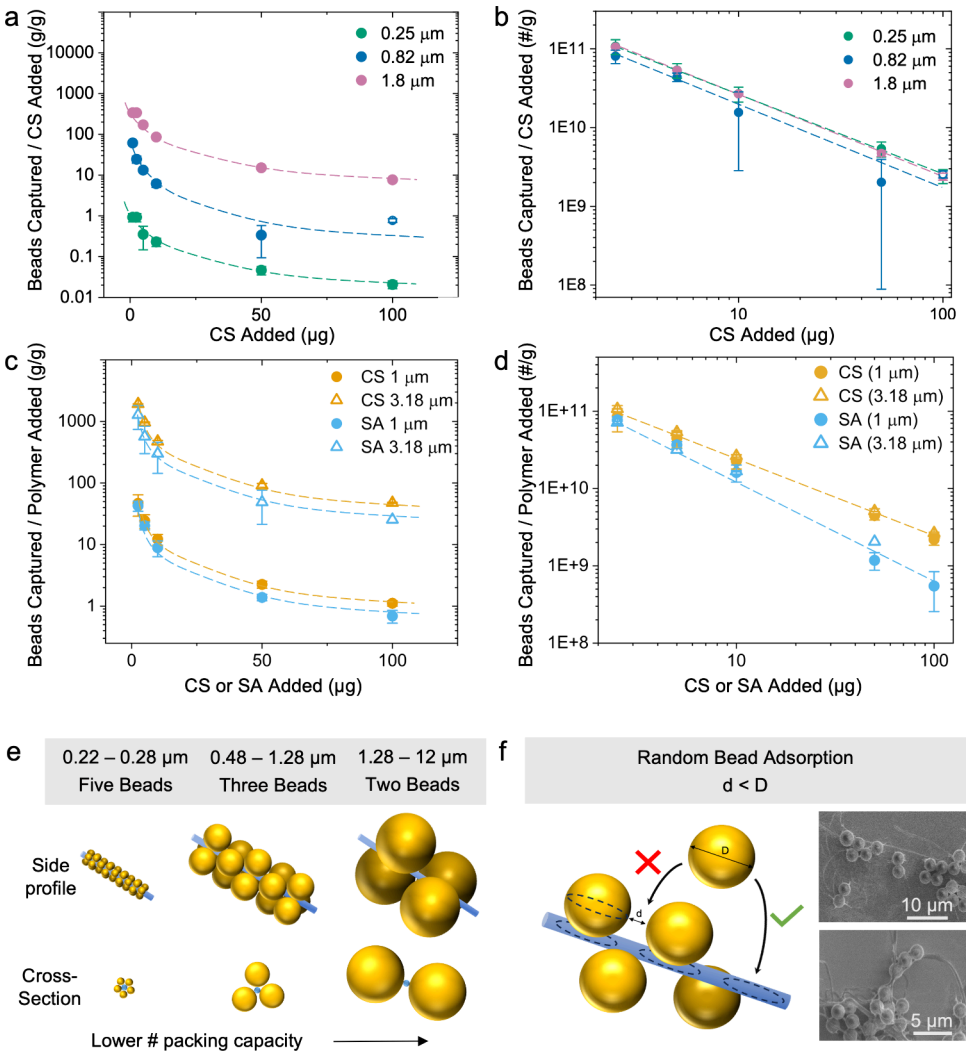

Figure 6. Effects of microbead size and charge on the collection by CS and SA hSDCs in 0.6 M NaCl suspensions. (a) Mass of microbeads captured per mass of dried CS hSDCs with increasing hSDC concentration. Dotted lines follow general data trends. (b) The number of latex microbeads captured per mass of CS hSDCs. (c) The mass of microbeads captured onto SA and CS hSDCs. (d) SA hSDCs capture a fewer number of microbeads compared to CS hSDCs. (e) Schematic of idealized bead packing for sizes that correspond to two, three, and five beads around an extended hSDC fiber of ~0.2 μm in diameter. S-PS and A-PS microbeads fall within these ranges. (f) Random bead adsorption will not allow maximum surface coverage as the bead spacing may hinder further bead adsorption, as shown by SEM image insets of microbeads entangled in CS SDCs in a less dense packing formation.

The effect of CS surface charge on the electrostatic interactions was investigated via microbead capture at varying pH without added salt, similar to other studies.[63] The zeta potential data, measured in a low-salinity medium (0.1 mM NaCl), listed in Table S1 and plotted in Figure 5b indicate an approximate isoelectric point of the CS hSDCs around pH 7. Excess surface charge below the isoelectric point leads to CS hSDCs with expanded conformations, and we observe a transition from expanded to an agglomerated hSDC conformation above the isoelectric point (Figure 5b). The agglomerated conformation is likely a result of neutralized amine groups and increased interparticle hydrogen bonding.[64,65] We expected that the dendricolloids would exhibit larger microbead adsorption under more acidic conditions since CS hSDCs would have a more positive zeta potential and expanded conformations. However, slightly more pronounced microbead collection was measured at higher pH conditions between 7.5 and 8.5 (Figure 5b). The lower microbead adsorption in more acidic conditions could result from possible swelling and higher hydration of the hSDCs.[62] Overall, the investigations in varying ionic media and pH levels suggest that vdW interactions play a predominant role. This explains the consistently high microbead capture across all tested ionic salt and pH range conditions.

Role of Microbead Size and Functional Groups in Microbead Capture. The next investigated key factor was the effect of microbead size on CS hSDC capture performance. One larger size and one smaller size S-PS microbead samples (0.25 and 1.8 μm, respectively) were tested alongside the 0.82 μm microbeads. The experiments were conducted at pH 8 and high-salinity conditions (0.6 M NaCl) to ensure electrostatic charge screening. CS hSDCs showed the highest level of capture of the 1.8 μm S-PS microbeads, collecting approximately 1000× more mass (g microbeads per g of dried CS) than 0.25 μm microbeads (Figure 6a). Yet, the number of microbeads absorbed per mass of CS was similar for all microbead sizes (power function slopes ~ −1.0 for 0.25, 1.8, and 0.82 μm, and slope of −1.3 for 0.82 μm if the data point

https://doi.org/10.1021/acs.langmuir.3c03869
Langmuir 2024, 40, 5923−5933

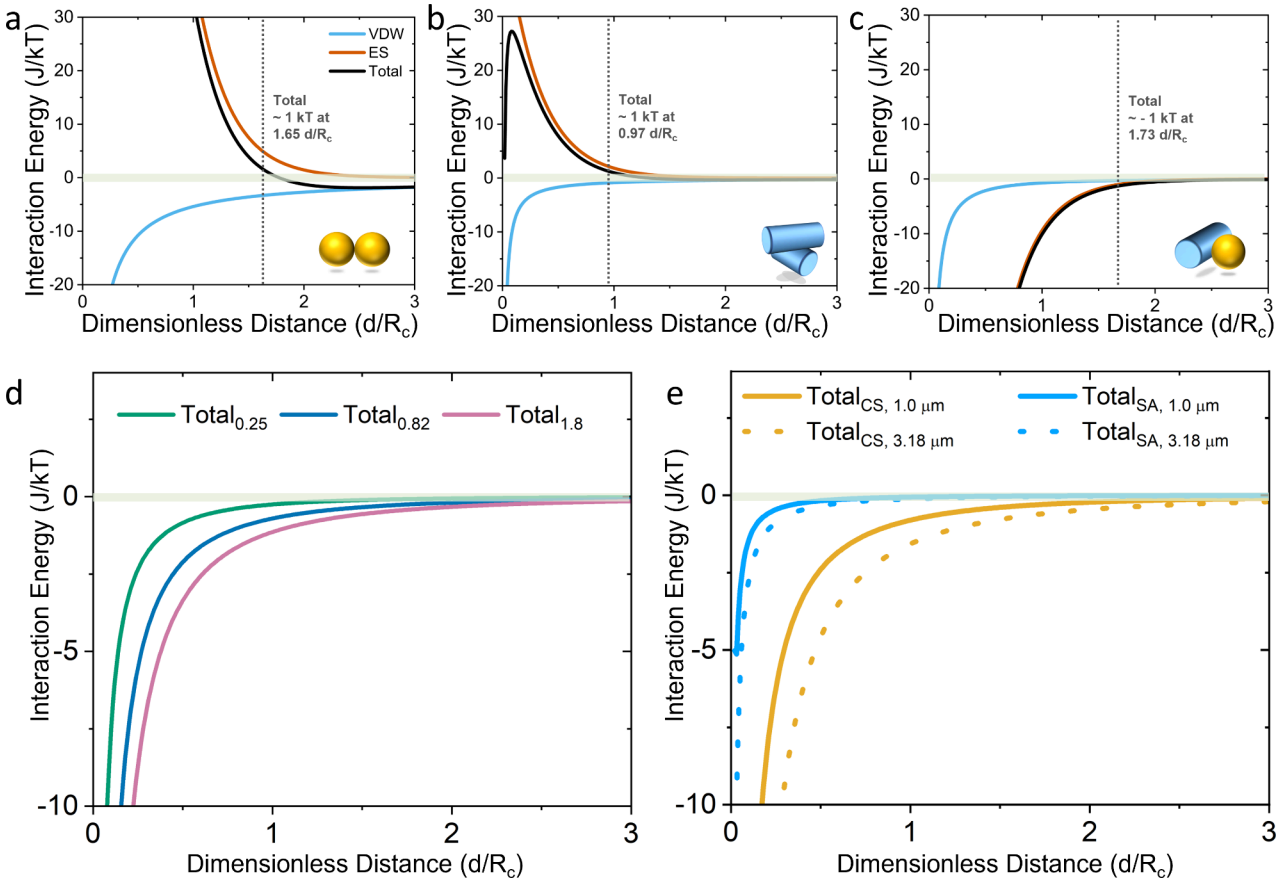

Figure 7. Evaluation by DLVO theory of the repulsive and attractive interactions in (a–c) 0.1 mM NaCl and (d–e) 0.6 M NaCl solutions. (a) Repulsive ES forces dominate over attractive vdW forces at short distances between two polystyrene microbeads. (b) The same is true for interactions between CS hSDC fibers modeled as crossed cylinders. (c) The interactions between the CS hSDCs and S-PS latex microbeads were approximated using a surface element integration (SEI) model from Li and Chen.[67] (d, e) Total interactions in a 0.6 M NaCl environment with different sizes of (d) sulfonated and (e) amidine-functionalized PS microbeads with (d, e) CS and (e) SA hSDCs.

for 100 μg CS hSDCs is omitted due to low sample number) (Figure 6b).

Amidine (A-PS) microbeads (1.0 and 3.18 μm diameters) were used to characterize the effect of surface functional groups on the microbead collection. Again, all samples were made under high-salinity conditions (0.6 M NaCl). Initially, pH conditions of 4 and 8, at which A-PS has a positive and negative charge, respectively (Table S1), were used to investigate the collection of 1 μm microbeads (Figure S5). SA hSDCs were compared to CS hSDCs to examine how their polymer composition affects microbead adsorption; results and discussion are given in the SI.

As expected, and similarly to the S-PS microbead collection result trends, both CS and SA hSDCs collected a greater mass of the larger A-PS microbeads (Figure 6c). Yet, when we compare the number of different-sized microbeads collected per gram of dry hSDC, we observe that the capture efficiency is similar when comparing the CS hSDCs (slopes of fitted power function ~ -1.0) and SA hSDCs (slopes of fitted power function ~ -1.3) (Figure 6d). We expected that the microbead size would affect the microbead packing around the SDC fibers and the number of adsorbed microbeads. However, this was not apparent when estimating the number of microbeads collected per unit mass of CS hSDC (Figure 6b,d). To estimate the maximal microbead adsorption amount onto the hSDCs, we evaluated the densest packing around the dendricolloid fibers for each microbead size by calculating the number of beads that would fit tightly around a cylinder (SI 1.3, Figure S6, and Table S2). The sphere–cylinder conformations for a number of microbead sizes are shown in Figure 6e. A maximum number of five microbeads of 0.25 μm diameter can pack tightly around a model fibril that is assumed to be of 0.2 μm diameter (based on image analysis of the outer SDC branches). Only two or three microbeads of 1.8 and 0.82 μm diameters, respectively, were able to fit around this fiber. While we did not expect the number of microbeads collected to be equal to the idealized maximal dense packing, as microbeads likely assume random packing configurations,[66] the densely packed model definitely did not match the experimentally observed trends.

The small difference in the number of captured microbeads of various sizes may be attributed to several factors. Rather than single-point adsorption as in the idealized particle "packing" model, fiber entanglement and wrapping around the microbeads or with each other, as seen in Figure 2c, may be more realistic. While the close packing model assumes beads tightly organized around a fiber (Figure 6e), random bead adsorption would hinder maximum surface coverage, as the already captured beads would not be optimally placed to allow for close-packed adsorption (Figure 6f). These results are consistent with SEM observations of adsorbed beads that allow for some gaps along the adsorbed chains and are entangled in multiple fibrils, as shown in the inset of Figure 6f and Figure S7.

https://doi.org/10.1021/acs.langmuir.3c03869
Langmuir 2024, 40, 5923–5933

While the packing model and trends from random sequential adsorption studies show increased surface area coverage as the bead diameter decreases,[66] the difference in surface area coverage may be insignificant with the range of microbead sizes tested. Although unexpected, the ability to collect the same number of microbeads regardless of size is an interesting finding that may aid in the further development of soft-matter MP cleaners.

Evaluations of Interactions Based on DLVO Theory. The attractive bead−SDC fibril interactions are obviously critical for microcleaner operation. We hypothesized that there is a competition of interactions between the SDC fibers (SDC−SDC) and microbeads (microbead−microbead) themselves. We used classical DLVO theory models to evaluate and compare the roles of the electrostatic and vdW interactions (the basis of DLVO models) within the system. The same fiber dimension (R_c = 0.1 μm diameter) used in the above packing model was used here.

We considered three types of colloidal interactions in our system: interactions between identical PS microbeads modeled with "sphere−sphere" geometry, interactions between SDC branches modeled with "crossed-cylinder" geometry, and two models for interactions between PS microbeads and SDC fibrils (Table S3). Common sphere−sphere and crossed-cylinder models[56] were used to calculate the interactions between the S-PS microbeads and the CS fibers, respectively. A constant-potential surface element integration (SEI) model by Li and Chen was used to describe more accurately the interactions between S-PS microbeads and CS fibers (Table S3 and Figure S8).[67] Other sphere−sphere models were also considered, and the differences between the different electrostatic approximations are seen in Figure S8. Ultimately, the SEI model was chosen as it is expected to better represent the interactions of a "sphere−cylinder" geometry with an opposite charge. The Hamaker constant (A_h), which dominates the vdW potential,[57] for the microbeads was approximated based on literature values.[58] The Hamaker constants, A_h, for the hydrogel SA and CS hSDCs were estimated by first approximating A_h for pure SA and CS from the materials' refractive indices (SI 1.4).

The evaluation of the interactions between microbeads (Figure 7a) and between SDCs (Figure 7b) shows that the electrostatic forces dominate over the vdW forces at short distances in low salt conditions. Both the electrostatic and vdW interactions in the system of microbeads and SDCs are attractive (Figure 7c). The microbeads and hSDCs are strongly attracted to each other and less attracted to themselves. The combined magnitude of bead−SDC fibril interaction energy is greater than the thermal energy, kT, below the dimensionless distance of 1.73 d/R_c, i.e., there will be sufficient attractive energies between the microbeads and hSDC fibers when the particles are closer than 0.173 μm from surface to surface.[68] Thus, once the microbeads closely approach the hSDC fibers, they will be captured irreversibly.

In the experiments reported in Figure 6 (0.6 M NaCl solution), the DLVO model showed dominant attractive vdW interactions and minimal electrostatic interactions due to charge screening (Figure 7d,e and Figure S9). The combined interactions between various sizes of S-PS microbeads and CS hSDCs show lower interaction with smaller microbead sizes. This may explain why the number of captured 0.25 μm beads is similar to that of the larger beads despite the potential for denser microbead packing. Furthermore, Figure 7e shows that SA hSDCs have lower vdW interactions with the microbeads due to the smaller A_h, as calculated for SA.

Overall, the DLVO theory provided insight and a feasible initial interpretation for the microbead capture results. It confirmed the competition of interactions between the two components in the system and confirmed the predominant contribution of the vdW interactions in media of high ionic concentrations. It also provided an explanation as to why agglomerated CS hSDCs performed better at higher pH conditions—agglomerated fibers may be "seen" as larger fibers by the microbeads, leading to larger vdW interactions (Figures S7 and S10). While DLVO does not account for all types of interactions that could take place in our model or in environmental samples, it provides a facile tool for initial data interpretation.

CONCLUSIONS

The results highlight the potential for using biodegradable soft dendritic colloids for the efficient collection of MPs. The hierarchical fibrillar morphology, large surface area, and attractive interfacial interactions of the dendricolloids enhance the adhesive capture and aggregation of large numbers of polymer microparticles. We found that CS hSDCs efficiently capture negatively charged S-PS microbeads in low- and high-salinity environments and across various pH conditions. The SDCs show similar performance in microbead collection to some commonly used flocculants in wastewater treatment plants.[69,70] However, the naturally derived CS SDCs are likely to be much less detrimental to aquatic life when used in open aquifers and may have the benefit of easier removal after microbead collection compared to that of the molecular flocculants. Additionally, we show that by the use of vdW forces, we can collect microbeads with a wide range of different functional groups and surface charges.

Interestingly, the amount of microbeads collected per gram of CS and SA hSDCs remained relatively constant with the size of the collected beads. Our hypothesis on the maximal packing efficiencies was not verified, as the results suggest that the microbeads may not have a single point of contact but rather become entangled or "wrapped" by the hSDC fibers (Figure S7). Alongside the empirical results, the consideration of the DLVO models points out that the vdW interactions are the dominant origin of attraction, especially at high-salinity conditions. Even in low salt concentration media, the overall attraction between the SDCs and the microbeads predominates the repulsive interactions between the SDC particles and microbeads themselves. Since the degree of branching controls the SDC properties that allow them to gel easily[43] and form pastes for 3D printing,[45] we expect that it can be used to further adjust the hSDC mode of action into specific types of polluted water.

Future work should be done to confirm the SDC's performance in collection of nanosized plastics and weigh in the influence of other MP surface properties, i.e., roughness or the presence of biofilm, on the collection efficiency. It is important to note that this paper reports data on the collection of monodisperse suspensions of model microbeads. It could be expected that the inherent polydispersity of real-world samples may affect the rate of microbead collection.[71,72] Thus, future investigations should consider methods of testing the hSDCs efficiency with polydisperse suspensions of microparticles.

The ubiquitous problems in MP remediation stem largely from the colloidal scale size of the nanodispersion and MP

https://doi.org/10.1021/acs.langmuir.3c03869
Langmuir 2024, 40, 5923−5933

dispersion.[28] We expect that the SDC microcleaners can circumvent the size limitations of many conventional methods of MP collection by using capture methods that harness the interfacial interactions in such systems. We hope our findings will help accelerate method development for water remediation, focusing on interfacial properties. Importantly, the use of bioderived and biodegradable matrixes for these microcleaners could lessen the environmental impact and carbon footprint of such MP cleanup procedures. The further development of MP cleaning processes based on SDC would require the inclusion of mechanisms for SDC dispersal, followed by their flotation to the surface after the capture of the MP targets. Our team is working on achieving these goals by means of active lateral and vertical motility of SDC microcleaners organized in supraparticle assemblies.

■ ASSOCIATED CONTENT

Supporting Information

The Supporting Information is available free of charge at https://pubs.acs.org/doi/10.1021/acs.langmuir.3c03869.

Separation of SDC−microbead aggregates and the "uncaptured" microbeads based on Stokes' law; Beer−Lambert law and the calculation of beads bound; approximating maximum microbead packing on SDC fiber; competition of interactions as described by DLVO; brightfield microscopy images and zeta potential values for CS and SA hSDCs; SEM images of the sedimentation; CS hSDC PS microbead (0.82 μm) absorption in salt and pure water; zeta potential values of S-PS and A-PS; microbead aggregation and sedimentation in varying salt concentrations; 1 μm A-PS microbeads absorbed by CS and SA hSDCs in suspensions with pH 4 and 8; densest packing schematic; densest packing of microbeads for an SDC fiber of 0.2 μm in diameter; different DLVO models used; SEM image of microbeads in less dense packaging formation; electrostatic interactions of microbead−SDC calculated by different models; interactions of S-PS beads in 0.6 M NaCl solution; and total interaction energy of single vs. aggregated fibers (PDF)

■ AUTHOR INFORMATION

Corresponding Author

Orlin D. Velev − *Department of Chemical and Biomolecular Engineering, North Carolina State University, Raleigh, North Carolina 27695, United States;* orcid.org/0000-0003-0473-8056; Email: odvelev@ncsu.edu

Authors

Rachel S. Bang − *Department of Chemical and Biomolecular Engineering, North Carolina State University, Raleigh, North Carolina 27695, United States*

Lucille Verster − *Department of Chemical and Biomolecular Engineering and Department of Forest Biomaterials, North Carolina State University, Raleigh, North Carolina 27695, United States*

Haeleen Hong − *Department of Chemical and Biomolecular Engineering, North Carolina State University, Raleigh, North Carolina 27695, United States*

Lokendra Pal − *Department of Forest Biomaterials, North Carolina State University, Raleigh, North Carolina 27695, United States*

Complete contact information is available at: https://pubs.acs.org/10.1021/acs.langmuir.3c03869

Author Contributions

O.D.V. and R.S.B. provided the initial conceptualization of this research and the methodology. R.S.B. and L.V. performed experimental research investigations and created the figures and visualization with the help of H.H. L.P. contributed to experimental analysis and assisted in providing feedback on the paper. Project funding was obtained by O.D.V., who also provided supervision and administration. R.S.B., L.V., and O.D.V. wrote the paper with feedback and assistance from all coauthors.

Author Contributions

#R.S.B. and L.V. contributed equally.

Funding

This study was supported by grants from the US National Science Foundation, EFMA-2029327 and partially CMMI-1825476. The visualization studies were performed in part at the Analytical Instrumentation Facility (AIF) at North Carolina State University, which is supported by the State of North Carolina and the National Science Foundation (award number ECCS-2025064). The AIF is a member of the North Carolina Research Triangle Nanotechnology Network (RTNN), a site in the National Nanotechnology Coordinated Infrastructure (NNCI).

Notes

The authors declare no competing financial interest.

■ ACKNOWLEDGMENTS

The authors are grateful to Drs. Carol Hall, Nathan Crook, Fengqi You, and Nicholas Abbott for their guidance and discussions. We also acknowledge Dr. Robert Kelly for providing a plate reader for absorbance measurements.

■ ABBREVIATIONS

MP/MPs	microplastics
GEC	global environmental change
NPs	nanoplastics
SDC	soft dendritic colloid
hSDC	hydrogel soft dendritic colloid
vdW	van der Waals
CS	chitosan
SA	sodium alginate
PS	polystyrene
S-PS	sulfonated polystyrene
A-PS	amidine-functionalized polystyrene
DLVO	Derjaguin−Landau−Verwey−Overbeek
DI	deionized
CA	cellulose acetate

■ REFERENCES

(1) Carr, S. A.; Liu, J.; Tesoro, A. G. Transport and Fate of Microplastic Particles in Wastewater Treatment Plants. *Water Res.* **2016**, *91*, 174−182.

(2) Hanvey, J. S.; Lewis, P. J.; Lavers, J. L.; Crosbie, N. D.; Pozo, K.; Clarke, B. O. A Review of Analytical Techniques for Quantifying Microplastics in Sediments. *Anal. Methods* **2017**, *9*, 1369−1383.

(3) Kik, K.; Bukowska, B.; Sicińska, P. Polystyrene Nanoparticles: Sources, Occurrence in the Environment, Distribution in Tissues, Accumulation and Toxicity to Various Organisms. *Environ. Pollut.* **2020**, *262*, No. 114297.

(4) Carpenter, E. J.; Smith, K. L. Plastics on the Sargasso Sea Surface. *Science* **1972**, *175*, 1240−1241.
(5) Tomaszewska, M.; Orecki, A.; Karakulski, K. Treatment of Bilge Water Using a Combination of Ultrafiltration and Reverse Osmosis. *Desalination* **2005**, *185*, 203−212.
(6) Brahney, J.; Mahowald, N.; Prank, M.; Cornwell, G.; Klimont, Z.; Matsui, H.; Prather, K. A. Constraining the Atmospheric Limb of the Plastic Cycle. *Proc. Natl. Acad. Sci. U.S.A.* **2021**, *118*, No. e2020719118.
(7) Allen, S.; Allen, D.; Phoenix, V. R.; le Roux, G.; Jiménez, P. D.; Simonneau, A.; Binet, S.; Galop, D. Atmospheric Transport and Deposition of Microplastics in a Remote Mountain Catchment. *Nat. Geosci.* **2019**, *12*, 339−344.
(8) Browne, M. A.; Galloway, T.; Thompson, R. Microplastic—an Emerging Contaminant of Potential Concern? *Integr. Environ. Assess. Manag.* **2007**, *3*, 559−561.
(9) Barrett, J.; Chase, Z.; Zhang, J.; Holl, M. M. B.; Willis, K.; Williams, A.; Hardesty, B. D.; Wilcox, C. Microplastic Pollution in Deep-Sea Sediments From the Great Australian Bight. *Front. Mar. Sci.* **2020**, *7*, No. 576170, DOI: 10.3389/fmars.2020.576170.
(10) Pabortsava, K.; Lampitt, R. S. High Concentrations of Plastic Hidden beneath the Surface of the Atlantic Ocean. *Nat. Commun.* **2020**, *11*, 4073.
(11) Browne, M. A.; Crump, P.; Niven, S. J.; Teuten, E.; Tonkin, A.; Galloway, T.; Thompson, R. Accumulation of Microplastic on Shorelines Woldwide: Sources and Sinks. *Environ. Sci. Technol.* **2011**, *45*, 9175−9179.
(12) Rochman, C. M.; Brookson, C.; Bikker, J.; Djuric, N.; Earn, A.; Bucci, K.; Athey, S.; Huntington, A.; McIlwraith, H.; Munno, K.; De Frond, H.; Kolomijeca, A.; Erdle, L.; Grbic, J.; Bayoumi, M.; Borrelle, S. B.; Wu, T.; Santoro, S.; Werbowski, L. M.; Zhu, X.; Giles, R. K.; Hamilton, B. M.; Thaysen, C.; Kaura, A.; Klasios, N.; Ead, L.; Kim, J.; Sherlock, C.; Ho, A.; Hung, C. Rethinking Microplastics as a Diverse Contaminant Suite. *Environ. Toxicol. Chem.* **2019**, *38*, 703−711.
(13) Andrady, A. L. Persistence of Plastic Litter in the Oceans. *Mar. Anthropog. Litter* **2015**, 57 DOI: 10.1007/978-3-319-16510-3_3.
(14) Peng, L.; Fu, D.; Qi, H.; Lan, C. Q.; Yu, H.; Ge, C. Micro- and Nano-Plastics in Marine Environment: Source, Distribution and Threats — A Review. *Sci. Total Environ.* **2020**, *698*, No. 134254.
(15) Alimi, O. S.; Farner Budarz, J.; Hernandez, L. M.; Tufenkji, N. Microplastics and nanoplastics in Aquatic Environments: Aggregation, Deposition, and Enhanced Contaminant Transport. *Environ. Sci. Technol.* **2018**, *52*, 1704−1724.
(16) Hwang, J.; Choi, D.; Han, S.; Jung, S. Y.; Choi, J.; Hong, J. Potential Toxicity of Polystyrene Microplastic Particles. *Sci. Rep.* **2020**, *10*, 7391.
(17) Yong, C.; Valiyaveettil, S.; Tang, B. Toxicity of Microplastics and nanoplastics in Mammalian Systems. *Int. J. Environ. Res. Public Health* **2020**, *17*, 1509.
(18) North, E. J.; Halden, R. U. Plastics and Environmental Health: The Road Ahead. *Rev. Environ. Health* **2013**, *28*, 1−8.
(19) Bank, M. S.; Mitrano, D. M.; Rillig, M. C.; Sze Ki Lin, C.; Ok, Y. S. Embrace Complexity to Understand Microplastic Pollution. *Nat. Rev. Earth Environ.* **2022**, *3*, 736−737.
(20) Gigault, J.; El Hadri, H.; Nguyen, B.; Grassl, B.; Rowenczyk, L.; Tufenkji, N.; Feng, S.; Wiesner, M. nanoplastics Are Neither Microplastics nor Engineered Nanoparticles. *Nat. Nanotechnol.* **2021**, *16*, 501−507.
(21) Hartmann, N. B.; Hüffer, T.; Thompson, R. C.; Hassellöv, M.; Verschoor, A.; Daugaard, A. E.; Rist, S.; Karlsson, T.; Brennholt, N.; Cole, M.; Herrling, M. P.; Hess, M. C.; Ivleva, N. P.; Lusher, A. L.; Wagner, M. Are We Speaking the Same Language? Recommendations for a Definition and Categorization Framework for Plastic Debris. *Environ. Sci. Technol.* **2019**, *53*, 1039−1047.
(22) Lim, X. Microplastics Are Everywhere - but Are They Harmful? *Nature* **2021**, *593*, 22−25.
(23) Cole, M.; Lindeque, P.; Halsband, C.; Galloway, T. S. Microplastics as Contaminants in the Marine Environment: A Review. *Mar. Pollut. Bull.* **2011**, *62*, 2588−2597.
(24) Al Harraq, A.; Brahana, P. J.; Arcemont, O.; Zhang, D.; Valsaraj, K. T.; Bharti, B. Effects of Weathering on Microplastic Dispersibility and Pollutant Uptake Capacity. *ACS Environ. Au* **2022**, *2*, 549−555.
(25) Hüffer, T.; Hofmann, T. Sorption of Non-Polar Organic Compounds by Micro-Sized Plastic Particles in Aqueous Solution. *Environ. Pollut.* **2016**, *214*, 194−201.
(26) Hüffer, T.; Weniger, A. K.; Hofmann, T. Sorption of Organic Compounds by Aged Polystyrene Microplastic Particles. *Environ. Pollut.* **2018**, *236*, 218−225.
(27) Filella, M. Questions of Size and Numbers in Environmental Research on Microplastics: Methodological and Conceptual Aspects. *Environ. Chem.* **2015**, *12*, 527−538.
(28) Bang, R. S.; Bergman, M.; Li, T.; Mukherjee, F.; Alshehri, A. S.; Abbott, N. L.; Crook, N. C.; Velev, O. D.; Hall, C. K.; You, F. An Integrated Chemical Engineering Approach to Understanding Microplastics. *AIChE J.* **2023**, *69*, No. e18020.
(29) Nguyen, B.; Claveau-Mallet, D.; Hernandez, L. M.; Xu, E. G.; Farner, J. M.; Tufenkji, N. Separation and Analysis of Microplastics and nanoplastics in Complex Environmental Samples. *Acc. Chem. Res.* **2019**, *52*, 858−866.
(30) Coppock, R. L.; Cole, M.; Lindeque, P. K.; Queirós, A. M.; Galloway, T. S. A Small-Scale, Portable Method for Extracting Microplastics from Marine Sediments. *Environ. Pollut.* **2017**, *230*, 829−837.
(31) Teh, C. Y.; Budiman, P. M.; Shak, K. P. Y.; Wu, T. Y. Recent Advancement of Coagulation-Flocculation and Its Application in Wastewater Treatment. *Ind. Eng. Chem. Res.* **2016**, *55*, 4363−4389.
(32) Mintenig, S. M.; Int-Veen, I.; Löder, M. G. J.; Primpke, S.; Gerdts, G. Identification of Microplastic in Effluents of Waste Water Treatment Plants Using Focal Plane Array-Based Micro-Fourier-Transform Infrared Imaging. *Water Res.* **2016**, *108*, 365−372.
(33) Zhao, S.; Zhu, L.; Gao, L.; Li, D. Limitations for Microplastic Quantification in the Ocean and Recommendations for Improvement and Standardization. In *Microplastic Contamination in Aquatic Environments: An Emerging Matter of Environmental Urgency*; Elsevier, 2018; pp 27−49 ISBN 9780128137475.
(34) Patrício Silva, A. L. New Frontiers in Remediation of (Micro)Plastics. *Curr. Opin. Green Sustain. Chem.* **2021**, *28*, No. 100443.
(35) Marichelvan, M. K.; Jawaid, M.; Asim, M. Corn and Rice Starch-Based Bio-Plastics as Alternative Packaging Materials. *Fibers* **2019**, *7*, 32 DOI: 10.3390/fib7040032.
(36) Kotb, Y.; Velev, O. D. Hierarchically Reinforced Biopolymer Composite Films as Multifunctional Plastics Substitute. *Cell Rep. Phys. Sci.* **2023**, *4*, No. 101732, DOI: 10.1016/j.xcrp.2023.101732.
(37) Al Harraq, A.; Bharti, B. Microplastics through the Lens of Colloid Science. *ACS Environ. Au* **2022**, *2*, 3−10.
(38) Singh, N.; Khandelwal, N.; Ganie, Z. A.; Tiwari, E.; Darbha, G. K. Eco-Friendly Magnetic Biochar: An Effective Trap for nanoplastics of Varying Surface Functionality and Size in the Aqueous Environment. *Chem. Eng. J.* **2021**, *418*, No. 129405, DOI: 10.1016/j.cej.2021.129405.
(39) Peydayesh, M.; Suta, T.; Usuelli, M.; Handschin, S.; Canelli, G.; Bagnani, M.; Mezzenga, R. Sustainable Removal of Microplastics and Natural Organic Matter from Water by Coagulation-Flocculation with Protein Amyloid Fibrils. *Environ. Sci. Technol.* **2021**, *55*, 8848−8858.
(40) Lapointe, M.; Farner, J. M.; Hernandez, L. M.; Tufenkji, N. Understanding and Improving Microplastic Removal during Water Treatment: Impact of Coagulation and Flocculation. *Environ. Sci. Technol.* **2020**, *54*, 8719−8727.
(41) Renault, F.; Sancey, B.; Badot, P. M.; Crini, G. Chitosan for Coagulation/Flocculation Processes - An Eco-Friendly Approach. *Eur. Polym. J.* **2009**, *45*, 1337−1348.
(42) Nabi, I.; Bacha, A. U. R.; Zhang, L. A Review on Microplastics Separation Techniques from Environmental Media. *J. Clean. Prod.* **2022**, *337*, No. 130458, DOI: 10.1016/j.jclepro.2022.130458.

https://doi.org/10.1021/acs.langmuir.3c03869
Langmuir 2024, 40, 5923−5933

(43) Roh, S.; Williams, A. H.; Bang, R. S.; Stoyanov, S. D.; Velev, O. D. Soft Dendritic Microparticles with Unusual Adhesion and Structuring Properties. *Nat. Mater.* **2019**, *18*, 1315−1320.
(44) Luiso, S.; Williams, A.; Petrecca, M. J.; Roh, S.; Velev, O. D.; Fedkiw, P. Poly(Vinylidene Difluoride) Soft Dendritic Colloids as Li-Ion Battery Separators. *J. Electrochem. Soc.* **2021**, *168*, No. 020517.
(45) Williams, A. H.; Roh, S.; Jacob, A. R.; Stoyanov, S. D.; Hsiao, L.; Velev, O. D. Printable Homocomposite Hydrogels with Synergistically Reinforced Molecular-Colloidal Networks. *Nat. Commun.* **2021**, *12*, 2834 DOI: 10.1038/s41467-021-23098-9.
(46) Williams, A. H.; Hebert, A. M.; Boehm, R. C.; Huddleston, M. E.; Jenkins, M. R.; Velev, O. D.; Nelson, M. T. Bioscaffold Stiffness Mediates Aerosolized Nanoparticle Uptake in Lung Epithelial Cells. *ACS Appl. Mater. Interfaces* **2021**, *13*, 50643−50656.
(47) Chou, T. C.; Fu, E.; Wu, C. J.; Yeh, J. H. Chitosan Enhances Platelet Adhesion and Aggregation. *Biochem. Biophys. Res. Commun.* **2003**, *302*, 480−483.
(48) Boido, M.; Ghibaudi, M.; Gentile, P.; Favaro, E.; Fusaro, R.; Tonda-Turo, C. Chitosan-Based Hydrogel to Support the Paracrine Activity of Mesenchymal Stem Cells in Spinal Cord Injury Treatment. *Sci. Rep.* **2019**, *9*, 6402.
(49) Shu, X. Z.; Zhu, K. J.; Song, W. Novel PH-Sensitive Citrate Cross-Linked Chitosan Film for Drug Controlled Release. *Int. J. Pharm.* **2001**, *212*, 19−28.
(50) Takeuchi, I.; Takeshita, T.; Suzuki, T.; Makino, K. Iontophoretic Transdermal Delivery Using Chitosan-Coated PLGA Nanoparticles for Positively Charged Drugs. *Colloids Surf., B* **2017**, *160*, 520−526.
(51) Ulery, B. D.; Nair, L. S.; Laurencin, C. T. Biomedical Applications of Biodegradable Polymers. *J. Polym. Sci. B. Polym. Phys.* **2011**, *49*, 832−864.
(52) Shariatinia, Z. Pharmaceutical Applications of Chitosan. *Adv. Colloid Interface Sci.* **2019**, *263*, 131−194.
(53) Rhim, J. W. Physical and Mechanical Properties of Water Resistant Sodium Alginate Films. *Food Sci. Technol.* **2004**, *37*, 323−330.
(54) Dalmoro, A.; Barba, A. A.; Lamberti, G.; Grassi, M.; d'Amore, M. Pharmaceutical Applications of Biocompatible Polymer Blends Containing Sodium Alginate. *Adv. Polym. Technol.* **2012**, *31*, 220−230.
(55) Ahmad, A.; Mubarak, N. M.; Jannat, F. T.; Ashfaq, T.; Santulli, C.; Rizwan, M.; Najda, A.; Bin-Jumah, M.; Abdel-Daim, M. M.; Hussain, S.; Ali, S. A Critical Review on the Synthesis of Natural Sodium Alginate Based Composite Materials: An Innovative Biological Polymer for Biomedical Delivery Applications. *Processes* **2021**, *9*, 137 DOI: 10.3390/pr9010137.
(56) Lacoste, C.; El Hage, R.; Bergeret, A.; Corn, S.; Lacroix, P. Sodium Alginate Adhesives as Binders in Wood Fibers/Textile Waste Fibers Biocomposites for Building Insulation. *Carbohydr. Polym.* **2018**, *184*, 1−8.
(57) He, Z.; Alexandridis, P. Nanoparticles in Ionic Liquids: Interactions and Organization. *Phys. Chem. Chem. Phys.* **2015**, *17*, 18238−18261.
(58) Israelachvili, J. *Intermolecular and Surface Forces*. 3rd ed., Elsevier Inc., 2011, ISBN 978−0-12−375182−9.
(59) Petosa, A. R.; Jaisi, D. P.; Quevedo, I. R.; Elimelech, M.; Tufenkji, N. Aggregation and Deposition of Engineered Nanomaterials in Aquatic Environments: Role of Physicochemical Interactions. *Environ. Sci. Technol.* **2010**, *44*, 6532−6549.
(60) Huh, J. H.; Kim, S. H.; Chu, J. H.; Kim, S. Y.; Kim, J. H.; Kwon, S. Y. Enhancement of Seawater Corrosion Resistance in Copper Using Acetone-Derived Graphene Coating. *Nanoscale* **2014**, *6*, 4379−4386.
(61) Gayen, P.; Saha, S.; Ramani, V. Selective Seawater Splitting Using Pyrochlore Electrocatalyst. *ACS Appl. Energy Mater.* **2020**, *3*, 3978−3983.
(62) Moncho-Jordá, A.; Adroher-Benítez, I. Ion Permeation inside microgel Particles Induced by Specific Interactions: From Charge Inversion to Overcharging. *Soft Matter* **2014**, *10*, 5810−5823.
(63) Jin, T.; Peydayesh, M.; Joerss, H.; Zhou, J.; Bolisetty, S.; Mezzenga, R. Amyloid Fibril-Based Membranes for PFAS Removal from Water. *Environ. Sci. Water Res. Technol.* **2021**, *7*, 1873−1884.
(64) Roy, J. C.; Salaün, F.; Giraud, S.; Ferri, A.; Chen, G.; Guan, J. *Solubility of Chitin: Solvents, Solution Behaviors and Their Related Mechanisms*. IntechOpen 2017, ISBN 978−953−51−3650−7.
(65) Berger, J.; Reist, M.; Mayer, J. M.; Felt, O.; Peppas, N. A.; Gurny, R. Structure and Interactions in Covalently and Ionically Crosslinked Chitosan Hydrogels for Biomedical Applications. *Eur. J. Pharm. Biopharm.* **2004**, *57*, 19−34.
(66) Memet, E.; Tanjeem, N.; Greboval, C.; Manoharan, V. N.; Mahadevan, L. Random Sequential Adsorption of Spheres on a Cylinder. *EPL* **2019**, *127*, 38004.
(67) Li, K.; Chen, Y. Evaluation of DLVO Interaction between a Sphere and a Cylinder. *Colloids Surf. A Physicochem.* **2012**, *415*, 218−229.
(68) Dissanayake, T. U.; Hughes, J.; Woehl, T. J. Dynamic Surface Chemistry and Interparticle Interactions Mediating Chemically Fueled Dissipative Assembly of Colloids. *J. Colloid Interface Sci.* **2023**, *650*, 972−982.
(69) Rajala, K.; Grönfors, O.; Hesampour, M.; Mikola, A. Removal of Microplastics From Secondary Wastewater Treatment Plant Effluent By Coagulation/Flocculation With Iron, Aluminum and Polyamine-Based Chemicals. *Water Res.* **2020**, *183*, No. 116045, DOI: 10.1016/j.watres.2020.116045.
(70) Tang, W.; Li, H.; Fei, L.; Wei, B.; Zhou, T.; Zhang, H. The Removal of Microplastics From Water By Coagulation: A Comprehensive Review. *Sci. Total Environ.* **2022**, *851*, No. 158224, DOI: 10.1016/j.scitotenv.2022.158224.
(71) Adamczyk, Z.; Siwek, B.; Zembala, M.; Weroński, P. Influence of Polydispersity on Random Sequential Adsorption of Spherical Particles. *J. Colloid Interface Sci.* **1997**, *185*, 236 DOI: 10.1006/jcis.1996.4540.
(72) Danwanichakul, P.; Charinpanitkul, T. Random Sequential Adsorption of Polydisperse Spherical Particles: An Integral-Equation Theory. *Phys. A* **2007**, *377*, 102 DOI: 10.1016/j.physa.2006.11.001.

https://doi.org/10.1021/acs.langmuir.3c03869
Langmuir 2024, 40, 5923−5933